

Square-Law Selector and Square-Law Combiner for Cognitive Radio Systems: An Experimental Study

Lucas Rodés^{*}, Ankit Kaushik^{*}, Shree Krishna Sharma[†], Symeon Chatzinotas[†], Friedrich Jondral^{*}

^{*}Communications Engineering Lab, Karlsruhe Institute of Technology (KIT), Germany

lucas.rodés@alu-etsetb.upc.edu, {ankit.kaushik, friedrich.jondral}@kit.edu

[†]SnT - securityandtrust.lu, University of Luxembourg, Luxembourg

{shree.sharma, symeon.chatzinotas}@uni.lu

Abstract—Cognitive Radio communication is foreseen as one of the possible candidates that can resolve spectrum scarcity currently faced by the upcoming wireless technologies. This scarcity can be solved by enabling secondary access to the licensed spectrum. The interference at the primary receiver can be avoided by employing a detector (spectrum sensing) at the Secondary Transmitter (ST). Energy detection is widely used due to its low complexity and applicability to a large range of primary user signals. Recently, antenna diversity techniques such as square-law selector and square-law combiner have been used to enhance the detection performance at the ST. In this context, the detector's performance pertaining to the antenna diversity techniques has been characterized analytically. However, issues such as RF impairments and deploying a fading model render hardware implementation of such techniques challenging. Motivated by this fact, this paper presents the deployment of a hardware, and subsequently utilize the theoretical expressions to validate the performance of a multi-antenna system at the ST that exploits antenna diversity techniques in a realistic environment. Finally, we emphasize the challenges faced during the hardware implementation and present our approach to address these challenges.

I. INTRODUCTION

Since its introduction by Mitola *et al.* in 1999 [1], Cognitive Radio (CR) communication is envisioned as one of the potential candidates that address the spectrum scarcity problem of future wireless networks. Spectrum sensing is mainly incorporated in the CR systems with a purpose of detecting the spectrum holes [2] in the Primary Transmitter (PT) spectrum. Several techniques such as energy detection, matched filter based detection, cyclo-stationary based detection and feature based detection have been studied to perform spectrum sensing [3]. Due to its low computational complexity and its versatility towards unknown Primary User (PU) signals, energy based detection is extensively investigated for performance analysis and subsequently preferred for hardware implementation.

It has been widely stated that the detector's performance largely contributes to the overall performance of the spectrum sensing based CR systems [4]. More importantly, it is essential to investigate scenarios that witness variations in the channel, specially at low Signal-to-Noise Ratio (SNR) situations. In order to address the channel fading, Digham *et al.* [5] and Herath *et al.* [6] proposed the implementation of conventional diversity techniques such as selection combining, equal-gain combining and maximum ratio combining. To this end,

Digham *et al.* [7] quantified the enhancement in the detector's performance by employing multiple antennas at the Secondary Transmitter (ST). Since these techniques, except for selection combining, require the knowledge of the phase of the PT signal, the complexity and the versatility (to sense different PU signals) of the energy detector is compromised.

In order to respect the low-complexity and the versatility of the energy detector, novel antenna diversity techniques (at the ST), such as Square-Law Selector (SLS) and Square-Law Combiner (SLC), were introduced [7], [8]. However, the performance analysis of the mentioned techniques has been limited to theoretical analysis. Besides this, in the literature [9], the PU signal is modeled as a Complex Symmetric Circularly Gaussian (CSCG¹) signal or a Constant Power (CP) signal by the secondary system. These signals closely resemble the waveforms such as Orthogonal Frequency Division Multiplexing (OFDM), which is used in IEEE 802.11 a/g/n/ac standards as well as in the state-of-the-art 3GPP standards (LTE and LTE-A), and Continuous Phase Modulation (CPM), which is largely employed in systems, such as, Global System for Mobile Communications (GSM) and DVB-RCS2 ETSI standard, respectively.

In context to the CR systems that employ antenna diversity, the analytical expressions of the detection probability and the false alarm probability, which characterize the performance of the detector, have been obtained for the Gaussian signal model only. However, the analytical expressions and consequently the performance analysis subject to the aforementioned antenna diversity techniques for the CP signal model is still lacking in the literature. In this regard, we complement the theoretical expressions performed in [7] for the CP signal model.

Besides the theoretical analysis, the implementation of antenna diversity techniques is a challenging task. As per the knowledge of the authors, the performance analysis of the antenna diversity techniques by means of a hardware deployment has not been considered in the literature. Motivated by this fact, we utilize the expressions of the detection probability and the false alarm probability for the Gaussian and the CP signals for the antenna diversity techniques and deploy these techniques on a real hardware, which is the main focus of the paper. Following the hardware implementation, we obtain the

¹Also referred as a Gaussian signal throughout the paper.

measurements to validate the performance of these techniques by comparing them with the theoretical expressions. Finally, we highlight the major challenges and propose solutions to facilitate the hardware deployment of the aforementioned techniques. These investigations can be essential for evolving the baseline models existing in the literature.

A. Contributions

In this paper, we provide the following contributions:

- We consider the deployment of a CR system that employs antenna diversity techniques (SLS and SLC) at the ST. Following the deployment process, we validate the expressions of false alarm probability and detection probability for the situations where the PU signal can be modeled as a CSCG and a CP signals.
- While the deploying hardware to obtain measurements, we outline the major challenges encountered during the experimental process and propose the respective solutions to these challenges. Particularly, the performance evaluation of the antenna diversity techniques requires the employment of a fading model, for instance, Rayleigh fading. From the perspective of hardware deployment, it is challenging² to realize the fading process. Due to this issues, the performance analysis of a spectrum sensing based CR systems by means of hardware implementation in context to channel fading has been rarely investigated in the literature. In this regard, we propose to emulate the fading process at the transmitter.

II. SYSTEM MODEL

We consider that the ST is equipped with L antennas and employs energy detection (spectrum sensing) to determine spectrum holes in the PU spectrum. The problem of determining the presence (\mathcal{H}_1) or absence (\mathcal{H}_0) of a PU signal by means of energy detection can be formulated as a hypothesis testing problem. The discrete and complex received signal at antenna l of the ST is given by

$$y_l[n] = \begin{cases} w_l[n] & \text{if } \mathcal{H}_0 \\ h_l x[n] + w_l[n] & \text{if } \mathcal{H}_1 \end{cases}, \quad (1)$$

where $w_l[n] \sim \mathcal{CN}(0, \sigma_{w_l}^2)$ denotes the received noise sample and $h_l \sim \mathcal{CN}(0, \sigma_{h_l}^2)$ stands for the channel gain. For each antenna, the discrete samples $x[n]$ at the PT, channel gain and the noise samples at antenna are assumed to be independent and identically distributed (i.i.d.) random variables, and are independent of each other.

The ST follows a slotted medium access such that the frame structure employs a periodic sensing [9]. According to which, the ST performs spectrum sensing for a duration τ followed by data transmission for each frame. The energy received

²The procedure of obtaining large number of realizations of the channel required for modeling the fading process is rather cumbersome. In addition, effects like correlated fading or measurements converging to a Nakagami- m fading model instead of Rayleigh fading model [10] cause deviation between the theoretical and empirical values.

evaluated over $N = f_s \tau$ samples is determined as $T(\mathbf{y}_l) = \frac{1}{N} \sum_{n=1}^N |y_l[n]|^2$, where f_s denotes the sampling frequency. $T(\mathbf{y}_l)$ represents the test statistic and $\mathbf{y}_l = [y_l[1] \dots y_l[N]]$ is the received signal vector at antenna l . In accordance with the multiple antenna system, the test statistic can be jointly represented as $[T(\mathbf{y}_1), \dots, T(\mathbf{y}_l), \dots, T(\mathbf{y}_L)]$. In the subsequent section, this joint test statistic is used to characterize the expressions of the false alarm probability and the detection probability at the ST.

III. THEORETICAL ANALYSIS

Here, we obtain the theoretical expressions of the detection P_d and false alarm probabilities P_{fa} for single antenna and multiple antenna systems, where the multiple antenna systems employ antennas diversity techniques namely: (i) SLS and (ii) SLC. The expressions obtained in this section are utilized to validate the experimental measurements obtained later in Section IV.

A. Single Antenna

We first present the expressions of P_d and P_{fa} for a certain antenna l . For large number of samples, the central limit theorem can be applied to approximate the distribution functions of $T(\mathbf{y}_l)$ corresponding to the underlying hypotheses by a Gaussian distribution [4]. The mean and the variance of $T(\mathbf{y}_l)$ corresponding to the different PU signal models and subject to underlying hypotheses are presented in Table I. Let $\gamma_l = |h_l|^2 P / \sigma_{w_l}^2$ be the SNR at antenna l , where $P = \frac{1}{N} \sum_{n=1}^N |x[n]|^2$ denotes the PT signal power over N samples. Clearly, γ_l incurs the variations due to channel fading, whose probability density function is given by

$$f_{\gamma_l}(\gamma_l) = \frac{1}{\bar{\gamma}_l} \exp\left(-\frac{\gamma_l}{\bar{\gamma}_l}\right), \quad (2)$$

where $\bar{\gamma}_l$ represents the expected SNR received at antenna l . The expressions of P_{fa} and P_d at antenna l are characterized as

$$P_{fa,l} = \mathcal{Q}\left(\frac{\lambda - \mu_{l|\mathcal{H}_0}}{\sigma_{l|\mathcal{H}_0}}\right), \quad (3)$$

$$P_{d,l} = \mathbb{E}_{\gamma_l} \left[\mathcal{Q}\left(\frac{\lambda - \mu_{l|\mathcal{H}_1}(\gamma_l)}{\sigma_{l|\mathcal{H}_1}(\gamma_l)}\right) \right],$$

where $\mathbb{E}_{\gamma_l}[\cdot]$ represents the expectation with respect to γ_l .

TABLE I
MEAN AND VARIANCE OF $T(\mathbf{y}_l)$ [9]

Scenario	CSCG	CP
$\mu_{l \mathcal{H}_0}$	$\sigma_{w_l}^2$	$\sigma_{w_l}^2$
$\sigma_{l \mathcal{H}_0}^2$	$\sigma_{w_l}^4 / N$	$\sigma_{w_l}^4 / N$
$\mu_{l \mathcal{H}_1}(\gamma_l)$	$\sigma_{w_l}^2(\gamma_l + 1)$	$\sigma_{w_l}^2(\gamma_l + 1)$
$\sigma_{l \mathcal{H}_1}^2(\gamma_l)$	$\sigma_{w_l}^4(\gamma_l + 1)^2 / N$	$\sigma_{w_l}^4(2\gamma_l + 1) / N$

B. Square-Law Selector (SLS)

According to this approach, the ST selects the antenna with the maximum received power. The test statistic at the output of the SLS is given by $\max\{T(\mathbf{y}_1), \dots, T(\mathbf{y}_L)\}$. In this regard, the false alarm and detection probabilities at the ST that employs SLS are characterized as

$$\begin{aligned} P_{\text{fa,SLS}} &= 1 - \prod_{l=1}^L (1 - P_{\text{fa},l}), \\ P_{\text{d,SLS}} &= 1 - \mathbb{E}_{\gamma_1, \dots, \gamma_L} \left[\prod_{l=1}^L (1 - P_{\text{d},l}(\gamma_l)) \right], \\ &= 1 - \int_0^\infty \dots \int_0^\infty \prod_{l=1}^L (1 - P_{\text{d},l}(\gamma_l)) f_{\gamma_l}(\gamma_l) d\gamma_l. \end{aligned} \quad (4)$$

where $\mathbb{E}_{\gamma_1, \dots, \gamma_L}$ represents the expectation with respect to $\gamma_1, \dots, \gamma_L$. The individual expressions of P_{fa} and P_{d} are characterized in (3).

C. Square-Law Combiner (SLC)

In this approach, the test statistic is determined by summing the outputs of the individual test statistics obtained from each antenna, i.e., $\sum_{l=1}^L T(\mathbf{y}_l)$. The test statistic at the output of the SLC follows a Gaussian distribution whose mean and variance are given by

$$\begin{aligned} \mu_{\text{SLC}|\mathcal{H}_0} &= \sum_{l=1}^L \mu_{l|\mathcal{H}_0}, \quad \mu_{\text{SLC}|\mathcal{H}_1}(\gamma_1, \dots, \gamma_L) = \sum_{l=1}^L \mu_{l|\mathcal{H}_1}(\gamma_l), \\ \sigma_{\text{SLC}|\mathcal{H}_0}^2 &= \sum_{l=1}^L \sigma_{l|\mathcal{H}_0}^2, \quad \sigma_{\text{SLC}|\mathcal{H}_1}^2(\gamma_1, \dots, \gamma_L) = \sum_{l=1}^L \sigma_{l|\mathcal{H}_1}^2(\gamma_l). \end{aligned} \quad (5)$$

Subject to the mean and the variance characterized in (5), the false alarm and the detection probabilities that employs SLC are characterized as

$$\begin{aligned} P_{\text{fa,SLC}} &= \mathcal{Q}\left(\frac{\lambda - \mu_{\text{SLC}|\mathcal{H}_0}}{\sigma_{\text{SLC}|\mathcal{H}_0}}\right), \\ P_{\text{d,SLC}} &= \mathbb{E}_{\gamma_1, \dots, \gamma_L} \left[\mathcal{Q}\left(\frac{\lambda - \sum_{l=1}^L \mu_{l|\mathcal{H}_1}(\gamma_l)}{\sum_{l=1}^L \sigma_{l|\mathcal{H}_1}(\gamma_l)}\right) \right]. \end{aligned} \quad (6)$$

IV. EXPERIMENTAL ANALYSIS

In this section, we present the experimental setup, which is used to obtain the measurements, necessary for the validation process. Besides this, we briefly discuss some of the major challenges faced while performing the hardware implementation. With this purpose, two USRPs B210 from Ettus Research [11], depicting the software radio platform, are deployed to realize the communication between the PT and the ST. GNU Radio installed at the host computers performs the baseband processing, refer to Fig. 1. To complement the validation process, the measurement data is analyzed offline using Matlab.

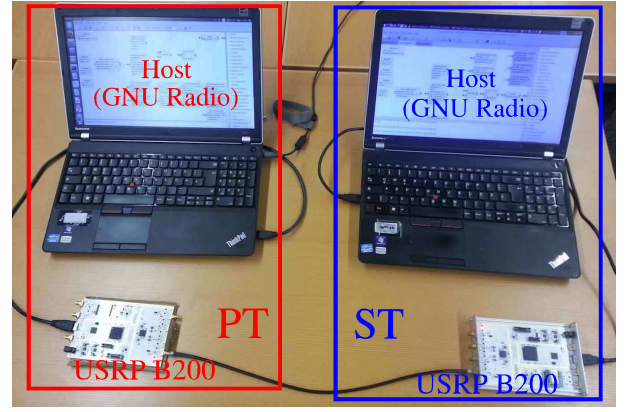


Fig. 1. Experimental setup: PT with emulated Rayleigh fading at the host computer (red) and ST with thermal noise and employment of band pass filter, digital mixing and down-sampling at the host computer (blue)

TABLE II
LIST OF PARAMETERS USED IN THE EXPERIMENTAL IMPLEMENTATION.

Notation	Definition	Value
f_c	Center frequency	2.422 GHz
f_{LOoffset}	Local Oscillator Offset frequency	55 kHz
f_s	Sampling frequency	150 kHz
N	Samples for sensing	100
τ_{est}	Estimation time for $\bar{\gamma}_l$ estimation	0.66 ms
N_{coh}	60% Coherence time (discrete)	3810
T_{coh}	60% Coherence time (continuous)	25.4 ms
B_{BF}	Bandpass filter bandwidth	30 kHz
M	Decimation factor	5
$\{\sigma_{w_l}^2\}_{l=1}^L = \sigma_w^2$	Noise power	-77.8 dBm

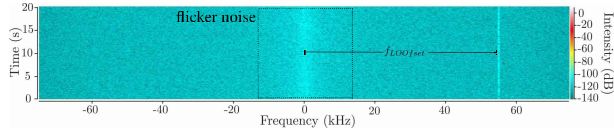
A. Modeling of OFDM and CPM signals

The Gaussian and the CP signals are used for modeling the PU signals, which correspond to the OFDM and the CPM signals, respectively. In practice, this modeling can be employed only if the sampling point is selected appropriately, hence resulting in i.i.d. samples. In other situations, the samples are correlated. This correlation is not considered while modeling the system, hence leads to deviation of the performance parameters (false alarm probability and detection probability) obtained theoretically from the ones obtained by performing the measurements. In order to resolve this issue, we propose to transmit the OFDM and CPM signals against their mathematical counterparts, these include a Gaussian and a sinusoidal signal, respectively. By doing this, we are able to avoid the correlation between the samples that are used for computing the energy.

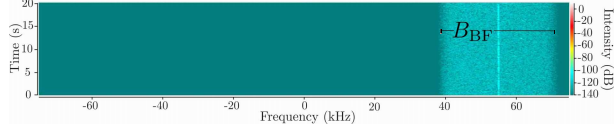
B. RF Imperfections

The USRP employed for realizing the antenna diversity represents a homodyne receiver³, hence, spurious effects such as flicker noise ($1/f$), DC offset and IQ imbalance are dominant, hence the validation process is influenced. These spurious effects, particularly, the DC offset and the flicker noise around the DC become significant at low SNR. In order

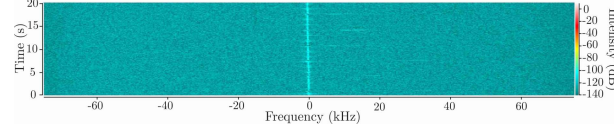
³A homodyne receiver implements a direct down conversion of a bandpass signal to the baseband.



(a) Received PT signal with DC offset at $f_{\text{LOOffset}} = 55$ kHz and flicker noise ($1/f$ noise)



(b) Signal after band pass filtering ($B_{\text{BF}} = 30$ KHz) at f_{LOOffset}



(c) Signal after digital down conversion and decimation

Fig. 2. Signal processing performed at the host computer to remove DC offset and flicker noise from the received signal.

to retrieve the samples close to those proposed while deriving the theoretical expressions (which does not take such spurious effects into account), following signal processing is proposed at the host computer.

- The received signal is oversampled (with sampling frequency 150 KHz, for a bandpass filter with bandpass frequency of 30 KHz applied, this corresponds to an oversampling factor of $M = 5$) and the local oscillator is tuned at a certain offset frequency defined as $f_{\text{LOOffset}} = 55$ KHz, refer to Fig. 2a.
- Subsequently, a bandpass filter (with bandwidth = 30 KHz) is employed to obtain the desired bandpass signal at f_{LOOffset} , which filters out the DC offset and the flicker noise present at low frequencies, cf. Fig. 2b.
- In order to obtain the low pass equivalent of the desired signal, a digital down conversion⁴ over the bandpass filtered signal is performed. In the end, decimation (refer to Fig. 2c) of the down converted signal is performed to reduce the correlation between the samples due to oversampling.

C. Estimation of Received SNR

Following the characterization of the P_d in (4) and (6) for the considered techniques, it is noticed that the knowledge of the receiver SNR $\bar{\gamma}_l$ (which is assumed to be perfectly known in the theoretical analysis) at the ST is essential. In this regard, as proposed in [12], received power estimation for each antenna is employed. Therefore, a certain time interval τ_{est} within the sensing time is allocated to the SNR estimation. Upon estimating $\bar{\gamma}_l$, it is possible to evaluate the detection probability for the deployed hardware. Table III presents the averaged (computed over different channel realizations of the channel for each antenna) value of the received SNR at each antenna for the different signal models.

⁴Multiplying a complex sinusoid with a frequency offset given by f_{LOOffset} .

TABLE III
ESTIMATED AVERAGE SNR AT EACH ANTENNA AT THE ST.

SNR	CSCG	CP
Antenna 1	-4.90 dB	-4.25 dB
Antenna 2	-4.82 dB	-4.21 dB
Antenna 3	-7.12 dB	-2.40 dB
Antenna 4	-3.95 dB	-2.29 dB

D. Emulating the fading environment

In order to validate the theoretical expressions for the antenna diversity techniques by means of measurements, it is important to realize the fading model, which considers uncorrelated (over the different energy measurements and across the antennas) Rayleigh fading. However, in practice, we may not encounter uncorrelated Rayleigh fading or the measurements may converge to a different fading model such as Nakagami- m fading model [10]. Due to these effects, hardware validation of the fading models is rarely considered. In order to facilitate the preliminary validation process, we propose the following simplification: The experiments are performed using a coaxial cable and Rayleigh fading is emulated at the PT.

By doing this, we establish a close relation between the analytical model and the acquired measurements, and consequently enhance the validation of a CR system that realizes channel fading and considers antenna diversity in a quasi-realistic situation. To proceed further with the hardware validation in a more realistic scenario, in future, it is essential to evolve the analytical model by taking correlated fading into account and determine the expression of the detection probability.

Now, to emulate fading at the ST, we modulate the transmit signal with $h^{(k)}x[n]$ at the PT using software, where $h^{(k)}$ represents the k -th realization of the channel gain. Energy is computed using N samples (sensing duration, τf_s). Since block fading is considered, the channel gain is assumed to remain constant over the sensing duration, that is, $N < N_{\text{coh}} = T_{\text{coh}}f_s$, N_{coh} represents the coherence time computed in samples. In order to obtain the value of T_{coh} (see Table II), we captured a signal by moving the ST by walking across the room. To avoid the shadowing effect, the measurements were restricted to a single room. Finally, a sequence of K PT signal modulated with the channel gain (which are randomly generated fading coefficients) is sent through a coaxial cable using a USRP, acting as PT. At the other end, another USRP, acting as the ST, receives the signal that consists of Rayleigh fading coefficients along the time domain.

E. Results

We finally complement the validation process by comparing the theoretical expressions of the detection and the false alarm probabilities, computed by inserting the parameters depicted in Table II, to the empirical (Emp) values that are obtained while performing the hardware measurements. Based on this validation, we understand the applicability of the solutions and the simplifications to the challenges proposed in sections IV-B, IV-A, IV-C and IV-D for the realization of the antenna diversity techniques over the hardware. Fig. 3 and Fig. 4

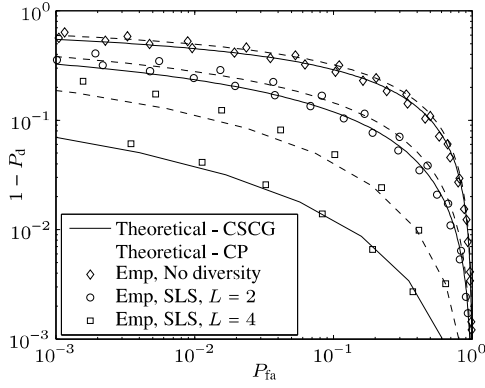


Fig. 3. Empirical (Emp) validation of the SLS antenna diversity technique, where $L \in \{1(\text{No diversity}), 2, 4\}$ for the CSCG (Gaussian) and CP signals.

illustrate the validation of the antenna diversity techniques with different: (i) signal models which include Gaussian (CSCG) and Constant Power (CP), (ii) antenna configuration $L = \{1(\text{No diversity}), 2, 4\}$.

We first consider the scenario, where the SLS is employed at the ST. Following the case where no diversity is employed (or $L = 1$), it is observed that the empirical results follow the analytical expressions for the considered signal models. It concludes that: (i) modeling of different signal models, (ii) baseband processing performed to reduce the effect of RF imperfections, (ii) estimation of the received SNR, required for characterizing the detection probability, and (iv) emulating the fading model results in accurate deployment of the fading channel. Therefore, the hardware setup is suitable for employing the antenna diversity techniques. Upon applying the SLS, it is noticed that the empirical values tend to deviate slightly from their theoretical counterparts as the number of antennas increases, particularly for $P_{fa} < 10^{-2}$.

This behaviour can be explained as follows: the performance due to the employment of antennas reduces the overlapping region between the two hypotheses, hence, the probabilities ($1 - P_d$ and P_{fa}) residing in these bins consist of low values. In this regard, a larger fluctuation due to the limited number of observations is expected. Besides this, SNR estimation (or the estimation error) could be responsible for the aforementioned deviation, which becomes significant as the system operates in a low probability regime. Next, the validation of the SLC is illustrated in Fig. 4. Clearly, an performance improvement compared to the SLS is noticed. Moreover, it is observed that the deviation between the empirical and the theoretical values compared to the SLS is reduced, specially for $L = 4$. It follows from the fact that the combined mean and variance (which are dependent on the estimated SNR) of the SLC are computed by adding the mean and variance of the individual antennas, hence, the estimation error is reduced.

V. CONCLUSION

In this paper, we considered the deployment of a CR system that employs spectrum sensing and antenna diversity techniques such as SLS and SLC at the ST. Particularly, the performance of such CR systems are validated by means of

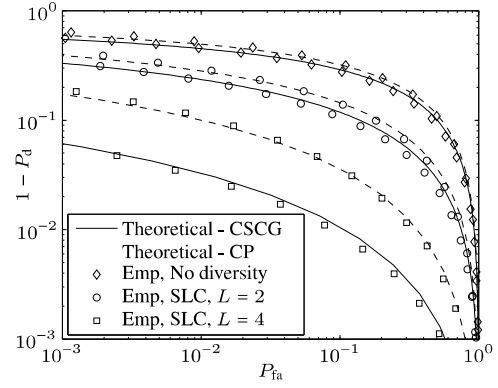


Fig. 4. Empirical (Emp) validation of the SLC antenna diversity technique, where $L \in \{1(\text{No diversity}), 2, 4\}$ for the CSCG (Gaussian) and CP signals.

hardware measurements. While deploying the hardware setup, major challenges such as modeling the PU signals, RF imperfections, SNR estimation and realizing the fading channel have been outlined and consequently simplifications and solutions have been proposed to facilitate the hardware realizability of the antenna diversity in a realistic scenario. In future, we plan to extend this work by relaxing the aforementioned simplifications. Particularly, in order to depict the feasibility of the CR systems in more realistic scenarios, we plan to incorporate correlated fading in the system model.

REFERENCES

- [1] J. Mitola and G. Q. Jr. Maguire, "Cognitive radio: making software radios more personal," *IEEE Personal Communications*, vol. 6, no. 4, pp. 13–18, August 1999.
- [2] A. Kaushik, M. Mueller, and F. K. Jondral, "Cognitive Relay: Detecting Spectrum Holes in a Dynamic Scenario," in *Proceedings of the Tenth International Symposium on Wireless Communication Systems (ISWCS 2013)*, Apr. 2013, pp. 1–2.
- [3] S. Sharma, T. Bogale, S. Chatzinotas, B. Ottersten, L. Le, and X. Wang, "Cognitive Radio Techniques under Practical Imperfections: A Survey," *IEEE Communications Surveys Tutorials*, vol. PP, no. 99, pp. 1–1, 2015.
- [4] R. Tandra and A. Sahai, "SNR Walls for Signal Detection," *IEEE Journal of Selected Topics in Signal Processing*, vol. 2, no. 1, pp. 4–17, Feb 2008.
- [5] F. Digham, M.-S. Alouini, and M. K. Simon, "On the energy detection of unknown signals over fading channels," in *IEEE International Conference on Communications (ICC)*, vol. 5, May 2003, pp. 3575–3579 vol.5.
- [6] S. Herath, N. Rajatheva, and C. Tellambura, "Energy detection of unknown signals in fading and diversity reception," *IEEE Transactions on Communications*, vol. 59, no. 9, pp. 2443–2453, September 2011.
- [7] F. Digham, M.-S. Alouini, and M. K. Simon, "On the energy detection of unknown signals over fading channels," *IEEE Transactions on Communications*, vol. 55, no. 1, pp. 21–24, Jan 2007.
- [8] S. K. Sharma, S. Chatzinotas, and B. Ottersten, "Spectrum sensing in dual polarized fading channels for cognitive satcoms," in *IEEE Global Communications Conference (GLOBECOM)*, 2012, pp. 3419–3424.
- [9] Y.-C. Liang, Y. Zeng, E. Peh, and A. T. Hoang, "Sensing-Throughput Tradeoff for Cognitive Radio Networks," *IEEE Transactions on Wireless Communications*, vol. 7, no. 4, pp. 1326–1337, April 2008.
- [10] A. Kaushik, M. R. Raza, and F. K. Jondral, "On the Deployment of Cognitive Relay as Underlay Systems," in *9th International Conference on Cognitive Radio Oriented Wireless Networks and Communications (CROWNCOM)*, Jun. 2014, pp. 329–334.
- [11] M. Ettus, "Ettus research, llc," *Online information on USRP board*, <http://www.ettus.com>, 2008.
- [12] A. Kaushik, S. K. Sharma, S. Chatzinotas, B. Ottersten, and F. K. Jondral, "Sensing-Throughput Tradeoff for Interweave Cognitive Radio System: A Deployment-Centric Viewpoint," *IEEE Transactions on Wireless Communications*, vol. PP, no. 99, 2016.